Acta Cryst. (1999). A**55**, 955–962

Tunable X-ray polarization reflector with perfect crystals

Y. Hasegawa,[a]*† Y. Ueji,[b] K. Okitsu,[c]‡ J. M. Ablett,[d] D. P. Siddons[d] and Y. Amemiya[a]†

[a]*Engineering Research Institute, University of Tokyo, Yayoi, Bunkyo, Tokyo 113, Japan ,* [b]*The Graduate University for Advanced Studies, Oho, Tsukuba, Ibaraki 305, Japan,* [c]*National Research Laboratory of Metrology, Umezono, Tsukuba, Ibaraki 305, Japan, and* [d]*NSLS, Brookhaven National Laboratory, Upton, NY 11973, USA.*
E-mail: yhaseg@kohsai.t.u-tokyo.ac.jp

(*Received 23 February 1999; accepted 21 May 1999*)

Abstract

The possibility of a transmission-type X-ray linear polarizer is investigated using a thin Bragg reflector as a polarizing filter. In this device, the transmitted beam (rather than the Bragg-reflected beam) is the useful output of the device. Consequently, the position and the direction of the transmitted beam are unchanged as the energy is changed, or even when the polarization direction to be filtered out is changed. Theoretical considerations as well as preliminary transmissivity measurements are presented. The use of perfect crystals of silicon and diamond is examined. A polarization ratio, defined as I_H/I_V, higher than 10^5 was observed in experiments to measure the performance characteristics of the proposed X-ray polarizing reflector. The transmission-type X-ray linear polarizer is well suited for spectroscopic measurements with polarized X-rays.

1. Introduction

Recently, polarization phenomena in the X-ray regime have been attracting attention. X-ray polarization effects are mainly due to the diffraction of the beam and/or the anisotropy of the susceptibility of the atom (Belyakov & Dmitienko, 1989). A variety of X-ray polarization phenomena was found to be involved in the scattering of X-rays at or near the absorption edge in atoms. Pioneering works were performed by Templeton *et al.* to show anisotropy of anomalous dispersion in an anisotropic crystalline environment (Templeton & Templeton, 1980, 1982, 1985). Pure and resonance magnetic scattering studies have also been reported (Brunel & de Bergevin, 1981; Namikawa *et al.*, 1985). With linearly polarized X-rays, observations of resonant X-ray optical activity and Faraday rotation of the plane of polarization were accomplished (Hart & Rodrigues, 1981; Siddons *et al.*, 1990; Hart *et al.*, 1991; Okitsu *et al.*, 1996). These experiments were made using a so-called X-ray polarimeter, *i.e.* an instrument consisting of a linear polarizer and a linear analyzer. Achieving an extremely high polarization extinction ratio at the crossed position (typically higher than 10^5) is important for X-ray polarimetric experiments, since it enables the detection of very small rotations of the plane of polarization, *e.g.* on the order of 10^{-3} or 10^{-4} rad. For spectroscopic measurements, it is necessary, in addition, to scan the energy of the beam over some range. For some experiments, it is also desirable to change the polarization direction.

The Thomson scattering amplitude depends on the polarization factor, P, which equals unity and $\cos 2\theta$, respectively for the σ- and π-polarization states. This predicts that single scattering at 90° (in the sense that the only scattering angle involved is 90°) produces a linearly polarized X-ray beam (Barkla, 1906; Compton & Allison, 1935). In particular, a Bragg reflection from a perfect crystal with a 45° Bragg angle provides high reflectivity and a high degree of polarization. Another method of obtaining a polarized X-ray beam is to utilize the anomalous transmission through a perfect crystal (Cole *et al.*, 1961). The former has a higher efficiency (almost 100%) than the latter owing to the well known region of total reflection of the Darwin curve for a perfect crystal. The polarization ratio, however, decreases quite rapidly with this reflection-type polarizer as the Bragg angle departs from exactly 45°. In particular, a polarization ratio higher than 10^3 can be achieved only in the small range $45 \pm 0.6°$ of the Bragg angle, resulting in a limited tunable energy range (Hart, 1978). The energy tunability was improved by the use of multiple reflections in an off-set channel-cut device (Hart & Rodrigues, 1979). This device still suffers from the disadvantage that the position of the reflected polarized beam moves depending on the energy of the beam and/or the polarization direction.

In this paper, we propose the possibility of filtering out one polarization state using a thin Bragg reflector. Thus, the transmitted beam is the useful output, which stays exactly at the same position and in the same direction when either the energy or the polarization

† Present address: Department of Applied Physics, University of Tokyo, Hongo, Bunkyo, Tokyo 113-8656, Japan.
‡ Present address: Engineering Research Institute, University of Tokyo, Yayoi, Bunkyo, Tokyo 113-8656, Japan.

ISSN 0108-7673

direction of the beam is changed. Theoretical considerations on the performance characteristics of the transmission-type polarizer are presented based on the dynamical theory of diffraction. This predicts a polarization ratio, defined as I_π/I_σ, higher than 10^6 with an output efficiency of more than 25%. Preliminary data from the transmissivity measurements of diamond and silicon polarizers are compared with theoretical predictions. In addition, experimental results show the performance of the polarization reflector with the use of a thin silicon plate, where we assumed the spectroscopic polarimetry experiment at the cobalt *K*-absorption edge.

2. Theory

The transmission-type polarizers that we describe must be fabricated from perfect crystals and the dynamical theory of diffraction describes their characteristics (Zachariasen, 1945; Batterman & Cole, 1964). This theory predicts a region of total reflection for a small range of angles near the Bragg angle. The angular width of this region is commonly called the Darwin width. This width depends on the polarization of the beam, *i.e.* the Darwin width for the π-polarized beam is cos 2θ times as much as that for the σ-polarized beam. In particular, when the crystal is set to satisfy the Bragg condition close to $\theta_B = 45°$, the reflected beam is mainly σ-polarized. On this basis, the conventional X-ray polarizer with multiple-reflection channel-cut structures selectively reflects a beam of one polarization state and this reflected beam is its useful output. A typical device would have two or four consecutive Bragg reflections. As a consequence, the output beam is offset from the input beam by a large amount, and this offset depends on the X-ray beam energy and the desired orientation of the output polarization vector. If, instead of the reflected beam, we concentrate on the properties of the transmitted beam during Bragg reflection, we find a complementary situation. Since the σ-polarized beam is totally reflected within the Darwin width, the remainder (*i.e.* the transmitted beam) is entirely π-polarized. This is exactly what we need, since the transmitted beam is polarized and always undeviated, *i.e.* its position and direction are always fixed regardless of the energy and the polarization direction of the output beam.

Rocking curves calculated from the dynamical theory of diffraction are shown in Fig. 1(*a*) for the transmitted beam through a silicon perfect crystal. Curves are shown for the σ- and the π-polarization states for the 422 symmetric reflection at 7.709 keV photon energy, *i.e.* at the cobalt *K*-absorption edge. This gives a Bragg angle $\theta_B = 46.5°$. The thickness of the plate in the calculation was varied from 40 to 100 µm in 20 µm steps. With the use of asymmetrically diffracting planes, it only changes the scale in the abscissas in addition to the effective thickness of the plates. Two features are worth mentioning here. The σ-polarized beam is almost entirely reflected out, there remaining less than 10^{-6} of the incident intensity at the center of the rocking curves. In contrast, in spite of attenuation by the absorption of the crystal, most of the π-polarized beam is transmitted in the range of Darwin's total reflection for the σ-polarized beam. Thus, the transmitted beam is expected to be highly π-polarized if the conditions for total reflection of the σ-polarized beam are satisfied. According to the calculation, a polarization ratio

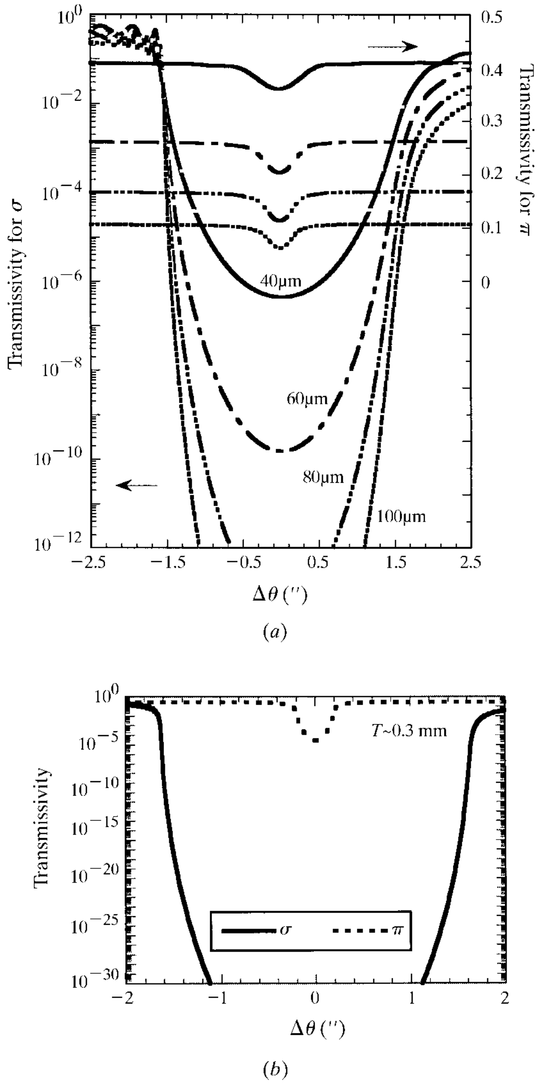

Fig. 1. Calculated rocking curves of a transmitted beam for (*a*) a silicon thin plate with symmetric 422 reflection and (*b*) a diamond plate with asymmetric 311 reflection at 7.709 keV photon energy. The thickness of the silicon plate is varied from 40 to 100 µm, whereas the thickness and the orientation of the diamond plate are assumed to be 0.3 mm and (100), respectively. The intensities of the transmitted beam are reduced in the total reflection range. In particular, the σ-polarized beam is expected to be extremely strongly reduced with diamond.

(defined as I_π/I_σ) higher than 10^6 can be obtained with an output efficiency of more than 25% using a silicon plate of 60 μm thickness. This value is sufficient in practice for X-ray polarimetric experiments.

Another candidate perfect crystal for the polarization reflector is diamond. Diamond perfect crystals are reported to be synthesized of good enough quality for use as X-ray optical elements, *e.g.* monochromators and phase retarders (Sumiya *et al.*, 1997; Hirano *et al.*, 1993, 1994, 1995). Diamond has the advantage of having a lower absorption coefficient than silicon, thus allowing us to use a thicker plate while maintaining a reasonable efficiency. In Fig. 1(*b*), the calculated transmitted-beam rocking curve for a diamond plate 300 μm in thickness is shown for the 311 reflection at 7.709 keV photon energy. This gives a Bragg angle $\theta_B = 48.4°$. The plate is assumed to be oriented with the [100] direction perpendicular to the surface, for which samples are practically available and results in the asymmetric factor b = 0.396. The σ-polarized beam is extremely strongly reduced in its Darwin total reflection region, whereas the π-polarized beam is attenuated to only about 30%. The transmissivity of the σ-polarized beam with the diamond plate is much less than with the silicon. This extremely low transmissivity is due to the fact that the lower absorption allows one to use a thicker plate, leading to a much higher extinction of the beam in the crystal.

The transmission-type X-ray linear polarizer proposed above produces a polarized beam for an incident beam within a limited angular divergence, *i.e.* in the Darwin total reflection range for the σ-polarized beam. In practice, the polarization ratio of the transmitted beam must be obtained with integrations of the transmissivity over the range of the angular divergence of the incident beam. The use of a synchrotron-radiation source is quite advantageous for such a device. In particular, the use of an undulator source would be optimal owing to its small angular divergence. For use at a bending-magnet beamline, the acceptance angle of the perfect crystal should be enlarged in some way. One of the easiest ways is the use of an asymmetric reflection by a perfect crystal. Another possibility is the use of multiple successive crystals with each one offset in angle with respect to the others. Although it is beyond the theoretical treatment here, a practical implementation of the transmission-type X-ray linear polarizer demands a higher perfection of the crystal, since even a small imperfection will make appreciable disturbances of the intensity in the transmitted direction.

3. Transmissivity measurement of silicon and diamond plates

As a preliminary, we measured the transmissivity of the σ-polarized beam with silicon and synthetic diamond perfect crystals at the Bragg condition. The experiments were carried out at a bending-magnet beamline, X12A at NSLS, Brookhaven National Laboratory. The experimental set-up is shown in Fig. 2. As a monochromator and an analyzer, four-bounce Si (422) channel-cut crystals were used. Either a single silicon

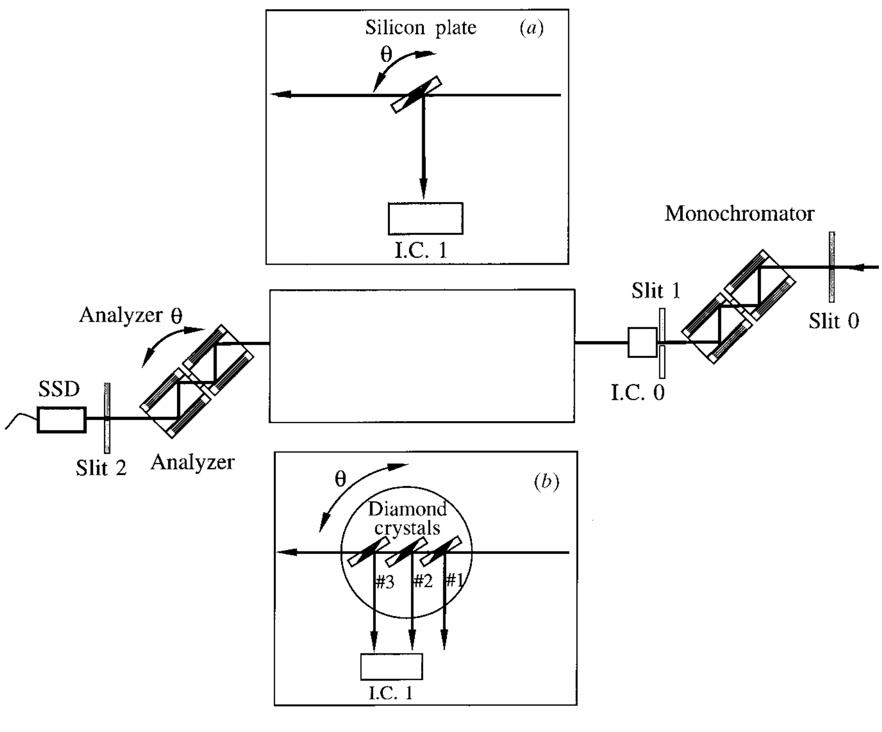

Fig. 2. Schematic view of the experimental set-up for the transmissivity measurements of (*a*) a silicon and (*b*) three successive diamond plates. As a monochromator and an analyzer, an Si (422) channel-cut crystal was used. The silicon or the diamond plate with slight off-set angles with respect to each other are inserted between the monochromator and the analyzer.

crystal or an assembly containing three successive diamond crystals with slight offset angles were inserted between the monochromator and the analyzer. The energy of the incident beam was tuned at the cobalt K-absorption edge, $E = 7.709$ keV, and the cross section of the beam was reduced to $0.8(V) \times 2.0(H)$ mm. A solid-state detector was set downstream of the analyzer. When required, Al foils were inserted before the detector in order to bring the beam intensity into its linear range. Two ion chambers were used to monitor the intensities of the primary beam and the reflected beam from the perfect crystals. We define θ as the angle that adjusts the crystals about the Bragg condition. The silicon plate was 15 µm in thickness and oriented in the [100] direction. This was aligned to give the 422 asymmetric reflection with an asymmetry factor $b = 0.197$, which gives the effective thickness of 75 µm.

Two different transmissivity measurements were performed using this silicon plate. In the first measurement, the monochromator and the analyzer were set parallel and the silicon plate was rotated around θ. The result of this measurement is shown in Fig. 3(a). Filled circles were measured with an absorber and the others were without it. Error bars in the measurement were within the symbols. The intensity of the beam was reduced to 1.6×10^{-5} when the plate was set on the Bragg condition. This confirmed that this Bragg reflector can considerably reduce the σ-polarized beam intensity as the theory predicted. In the second measurement, the analyzer was rotated with the silicon plate on the Bragg condition. Fig. 3(b) shows the result of this analyzer $\Delta\theta$ scan. This profile shows the angular distribution of the beam after passing through the four-bounce Si (422) channel-cut monochromator and the Si (422) asymmetric reflector. A dip is seen at the center of the profile, which is due to the fact that, at this angle, the primary beam was filtered out by the total reflection at the silicon plate. As a consequence, this dip generates two weak peaks, one on either side. One has 61 times and the other 13 times as much intensity as the bottom. They are already more than 4 orders of magnitude below the primary beam and are considered to result from the tail of Darwin's total reflection region of the four-bounce Si monochromator and analyzer. The asymmetry of the peaks is attributed to the fact that the lower-angle peak comes from tie points on the α-branch of the dispersion surface with lower absorption, whereas the higher-angle peak comes from the β-branch with higher absorption.

The diamond perfect-crystal samples were 0.3 mm in thickness and were oriented in the [100] direction. In order to increase the acceptance angle, we decided to place three crystals successively in the primary beam. They were aligned such that the Bragg peak from each one was separated roughly 2″ from its neighbour. The 311 asymmetric reflections were used, which additionally increased the acceptance angle (asymmetry factor $b = 0.396$). At first, θ of the diamond crystals were varied with the off-set angles constant. The results of the $\Delta\theta$ scan of diamond is shown in Fig. 4(a). The intensity of the transmitted beam was reduced to only 5×10^{-3}, whereas the theory predicts a value of much less than 10^{-8}. The observed value is not low enough for this arrangement to be useful as a transmission-type polarizer. In order to analyze the angular distribution of the transmitted beam, the throughput intensity was measured as a function of the analyzer angle, *i.e.* similar to the measurement in Fig. 3(b). The result is shown in Fig. 4(b). Here, it is seen that a significant amount of the beam was still transmitted in the primary-beam direction. This is the origin of the higher transmissivity than predicted by the theory. The deviation in the transmissivity measurements from the theoretical prediction is considered mainly due to imperfections in the diamond crystal samples which were available for these experiments.

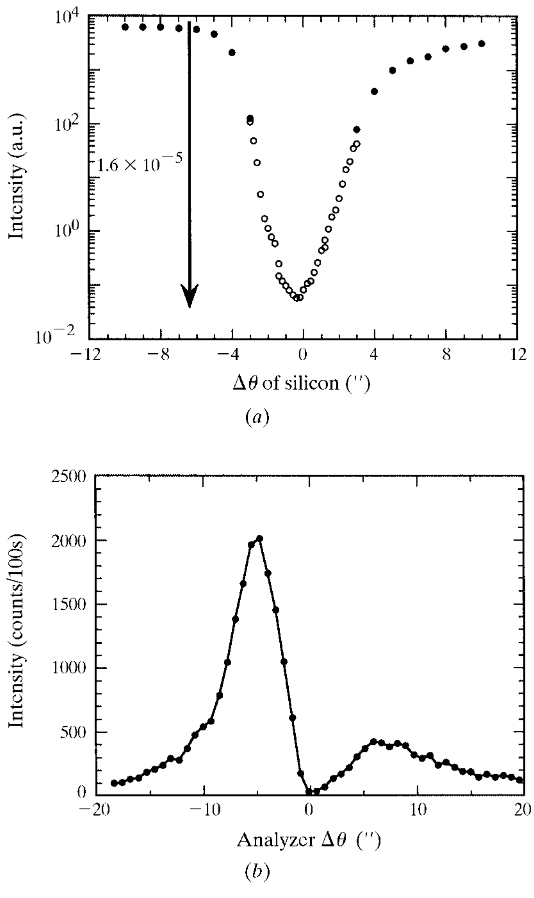

Fig. 3. Results of the transmissivity measurements of the silicon thin plate. (a) The $\Delta\theta$ scan of the silicon plate. Filled circles were measured with an absorber and the others were without it. The intensity of the transmitted beam was reduced to 1.6×10^{-5} when the plate was set on the Bragg condition. (b) The analyzer $\Delta\theta$ scan. Keeping the plate on the Bragg condition, the throughput intensity was analyzed with rotating the analyzer. The bottom of the dip is at the analyzer position parallel to the monochromator.

4. Performance of the transmission-type X-ray linear polarizer

Preliminary data from the transmissivity measurements suggested that the silicon plate was acceptable for use as a transmission-type polarizer, whereas the quality of the diamond crystals is still not high enough. Therefore, we decided to use the silicon perfect crystal in the following experiments to show the performance characteristics of the transmission-type polarizer. A schematic view of the experimental setup is shown in Fig. 5. An Si (111) channel-cut monochromator was placed upstream of the silicon thin-plate polarizer. First of all, the energy of the incident beam was tuned at the cobalt K-absorption edge, E = 7.709 keV, and the beam size was set to $0.5(V) \times 1.0(H)$ mm. An ion chamber (omitted in the drawing) was inserted after the monochromator to monitor the primary-beam intensity. The silicon polarizer was the plate used in the preliminary experiment and the same 422 asymmetric reflection was used. As an analyzer, an off-set Si (422) channel-cut crystal with four-bounce reflections was placed after the polarizer, whose performance as an analyzer had been established earlier. This analyzer was set near the crossed position with respect to the polarizer and was rotated around the primary-beam direction, *i.e.* a χ scan, so as to investigate the performance of the transmission-type polarizer. A solid-state detector was set downstream of the analyzer. In our experimental set-up, the polarizer produced a horizontally polarized beam and the analyzer selected the remaining vertically polarized beam. For the characterization of the transmission-type X-ray linear polarizer, the polarization state of the outgoing beam from the polarizer was determined by the analyzer χ scan. There, the intensity of the polarized X-rays transmitted through the analyzer is expected to be modulated as

$$I \cong (I_0/2)(1 - M\cos 2\chi), \qquad (1)$$

where I_0, M and χ are the intensity of the primary beam, modulation ratio and the angular position of the analyzer with respect to the electric vector of the incident polarized beam, respectively. The polarization ratio, defined as I_H/I_V, is given with this modulation ratio, M, by

$$I_H/I_V = (1 + M)/(1 - M). \qquad (2)$$

In order to show qualitatively the performance of the polarizer, analyzer $\Delta\theta$ scans were made for several χ positions. The production of a polarized beam with the polarizer on the Bragg condition should result in a decrease of the throughput beam intensity, which should depend on the χ position. We set the polarizer on the Bragg condition and the analyzer was rotated around the normal axis to the beam to satisfy the Bragg condition, *i.e.* $\Delta\theta$ scan. In Fig. 6, the analyzer $\Delta\theta$ scans are shown at several χ positions. Here, dips are due to the removal of the σ-polarized beam and the deepest dip was accomplished when the polarizer and the analyzer

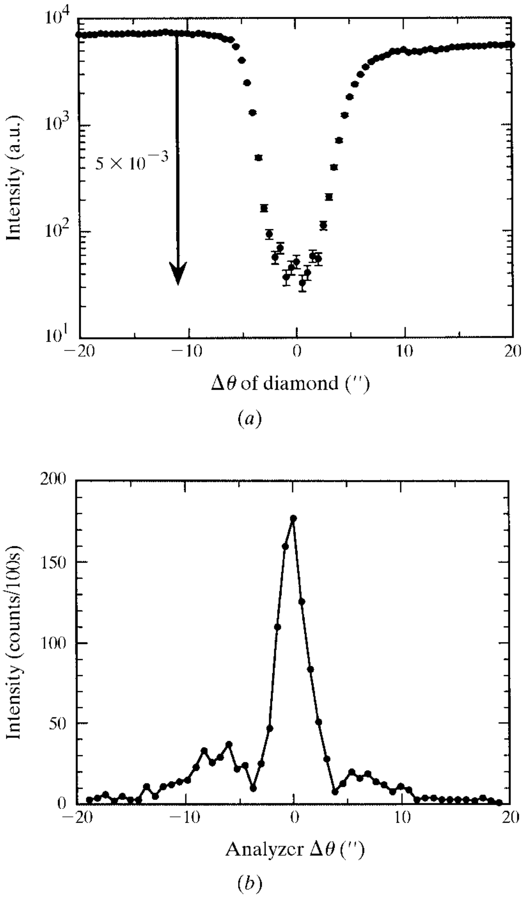

Fig. 4. Results of the transmissivity measurements with diamond crystals. (a) The $\Delta\theta$ scan of the diamonds. The intensity of the transmitted beam was reduced to 5×10^{-3} at most, even when the diamond crystals were set on the Bragg condition. (b) The analyzer $\Delta\theta$ scan. The throughput intensity was measured with the diamond crystals at the Bragg condition. When the analyzer was set on the Bragg condition, an excessive amount of the beam was still transmitted. This is considered to be due to the imperfection of the diamond crystals used here.

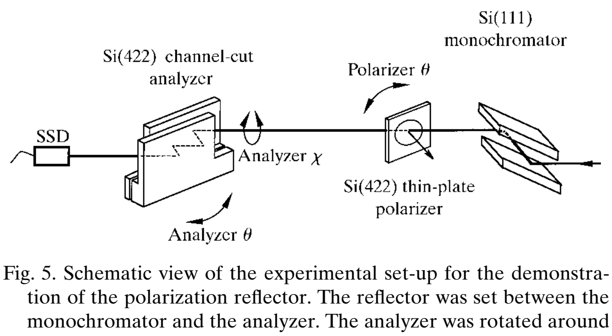

Fig. 5. Schematic view of the experimental set-up for the demonstration of the polarization reflector. The reflector was set between the monochromator and the analyzer. The analyzer was rotated around the primary-beam direction to determine the degree of polarization.

were set at the crossed position. The minimum throughput intensities of the analyzer $\Delta\theta$ scan are expected to modulate sinusoidally as a function of the rotation angle χ [see equation (1)]. In particular, it shows approximately parabolic behavior near the crossed position to the polarizer. In Fig. 7, the minimum throughput intensities in the analyzer $\Delta\theta$ scans are plotted with the least-squares fits of a sinusoidal curve as a function of χ. After obtaining the modulation ratio, M in equation (1), from the fitting parameters, the polarization ratio, defined as I_H/I_V, was calculated to be 1.75×10^5. This extinction ratio is consistent with the preliminary data and implies that our transmission-type polarizer works quantitatively well. In the final stage of the experiments, the energy of the incident beam was changed around the cobalt K-absorption edge. Here, since we assumed the spectroscopic measurement with the X-ray polarimeter, the energy was tuned ΔE = [−7 eV, 3.5 eV] near the cobalt K-absorption edge. The analyzer χ scans with least-squares fits at several energies of the incident beam are shown in Fig. 8 together with the obtained values of the polarization ratio. In all cases, a polarization ratio in excess of 10^5 was accomplished. This confirmed that our transmission-type polarizer achieves a level of performance that is more than adequate for polarized X-ray spectroscopic measurements.

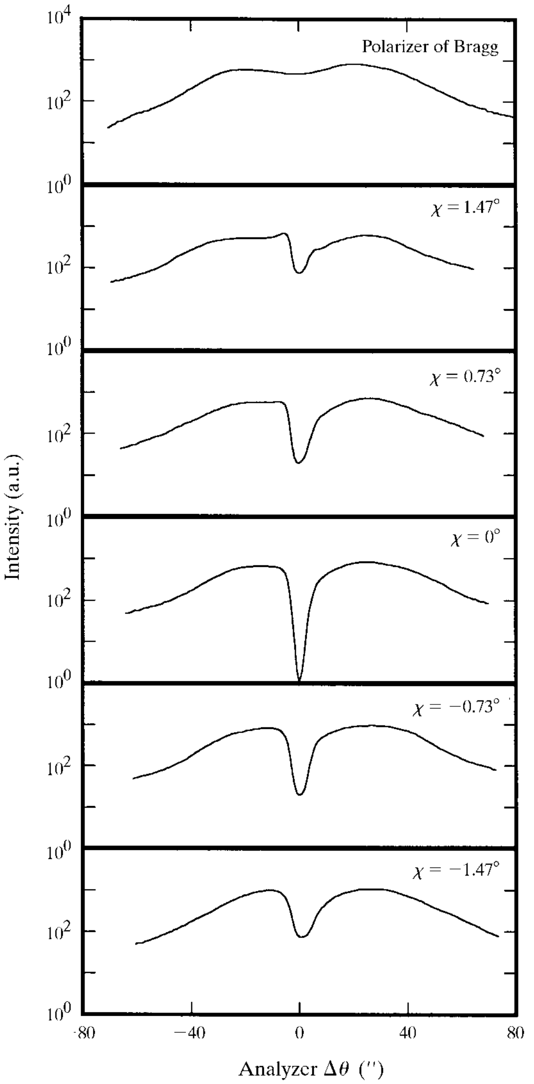

Fig. 6. Typical analyzer $\Delta\theta$ scan with several rotation angles, χ, of the analyzer. Dips are seen owing to the removal of the beam of one polarization state, showing that the transmitted beam is polarized.

5. Discussion

As described in §2, the acceptance angle for the polarization reflector should be enlarged in some way. Two possibilities were shown in our experiments: the use of an asymmetric reflection and successive multiple crystals with certain off-set angles with respect to the other. In both cases, the thicker the effective thickness of the plate(s) for the transmitted beam, the lower the efficiency of the polarizer becomes owing to the higher attenuation of the useful beam by the plate(s). In the case of the silicon plate, the efficiency of the polarizer, the transmissivity of the π-polarized beam, reached more than 20%. This value is comparable to the conventional X-ray linear polarizer with multiple-

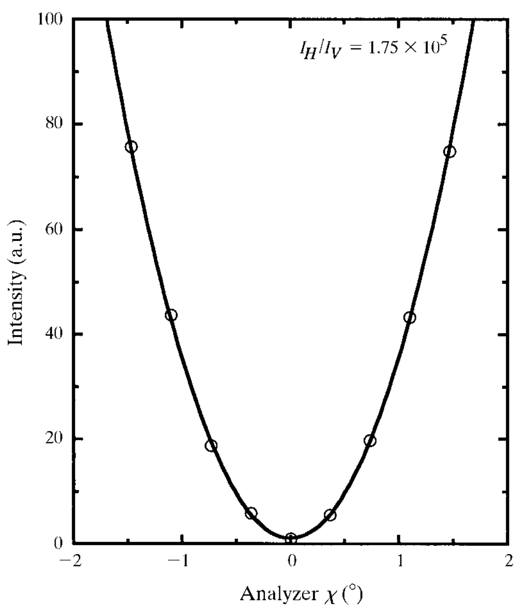

Fig. 7. The minimum throughput intensity in the analyzer $\Delta\theta$ scan is plotted with the least-squares fit as a function of the rotation angle, χ, of the analyzer. The polarization ratio, defined as I_H/I_V, is calculated to be 1.75×10^5.

reflection channel-cut structure. In order to investigate another possibility to achieve higher efficiency, we tried to use diamond perfect crystals with lower attenuation than silicon. This was not successful owing to the imperfection of the diamond crystals used here, as we found in the preliminary data from the transmissivity measurements. There is, however, still a possibility that, in the future, diamond perfect crystals of adequate quality will become available. In that case, a higher efficiency of the transmission-type polarizer can be realized.

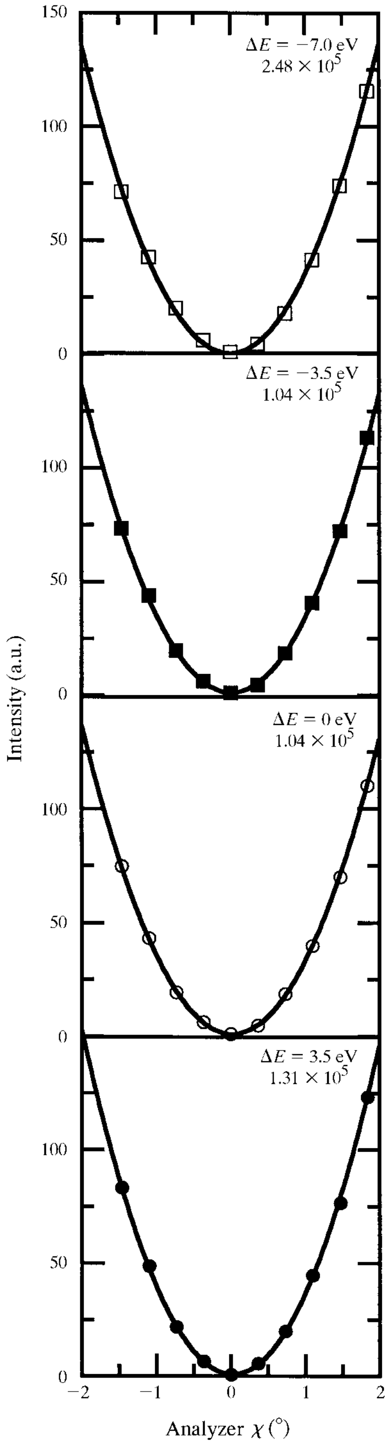

Fig. 8. The analyzer χ scans with least-squares fits at several energies of the incident beam together with calculated values of the polarization ratio. In all cases, a polarization ratio in excess of 10^5 was obtained.

In these experiments, a polarization ratio on the order of 10^5 was obtained. On careful consideration, we recognize the fact that this accomplishment is partially due to the initial polarization of the incident beam from the synchrotron radiation. In our case, the polarization ratio of the incident beam was estimated to be 20 to 50 and the effectiveness of the transmission-type polarizer was on the order of 10^4 (see Fig. 6). This value is well justified by the about 20% efficiency of the polarization reflector and the 1.6×10^{-5} transmissivity for the σ-polarized beam of the silicon plate used here. A higher polarization ratio demands a further transmissivity reduction of the reflector. It is worth noting here that the obtained extinction value in the transmissivity measurement already deviates from that predicted by the theory. As is apparent in the profile of the analyzer $\Delta\theta$ scan in the transmissivity measurement, *i.e.* Fig. 3(*b*), this deviation is regarded as being mainly due to an unwanted transmission of the beam on the tail of the Darwin total-reflection region. Thus, the reduction of this transmission on the tail can improve the polarization ratio considerably. One possibility to reduce this unwanted signal is to reduce the angular acceptance of the analyzer by the use of an asymmetric reflection.

The proposed as well as the conventional polarizer utilizes the property of the narrow and the wide Darwin total-reflection regions for the π- and σ-polarized beams. The deviation of the Bragg angle from exactly 45° decreases only the efficiency of the proposed transmission-type polarizer by a factor, whereas it decreases the polarization ratio of the conventional reflection-type polarizer by an order of magnitude. Thus, the energy tunability with the polarization ratio, say in excess of 10^5, with the transmission-type polarizer is much wider than with the reflection-type polarizer. This would be useful for applications at other absorption edges.

Attention should be paid to the fact that the polarization reflector is best used in combination with an appropriate collimator or filter, since it works well only over a small angular divergence region. This is best achieved with the use of parallel reflection planes for the reflector and the collimator/filter, when the effect of dispersion is removed. Considering this point and the polarization ratio obtained so far, one of the good prospects with the polarization reflector is a polarizer combined with a generally equipped Si(111) (pre)-monochromator followed by an appropriate analyzer/filter.

6. Conclusions

We have proposed a transmission-type X-ray linear polarizer with perfect crystals, *e.g.* silicon or diamond. The diamond crystals obtained so far were not suitable for use in the polarization reflector owing to their imperfections, which resulted in a high transmissivity of the σ-polarized beam. We have successfully fabricated a polarization reflector using a thin silicon plate and demonstrated its performance characteristics. In our experiments, a polarization ratio higher than 10^5 was accomplished over the energy range ΔE = [−7 eV, 3.5 eV] near the cobalt *K*-absorption edge. This transmission-type polarizer has the advantages of a wider energy tunability in addition to the fact that the position and the direction of the useful output beam are stationary when the energy is changed or even when the polarization direction to be filtered out is changed. These characteristics are very desirable for spectroscopic measurements with polarized X-rays.

The present work was partly supported by a Grant-in-Aid for COE Research and Scientific Research from the Ministry of Education, Science and Culture, Japan. Work at NSLS was supported by the US Department of Energy under contract No. DE-AC02-76CH00016. YH would like to thank Dr S. Nakatani (ISSP, Japan) for help in the preparation of the thin silicon plates.

References

Barkla, C. G. (1906). *Proc. R. Soc. London Ser. A*, **77**, 247–250.
Batterman, B. W. & Cole, H. (1964). *Rev. Mod. Phys.* **36**, 681–717.
Belyakov, A. V. & Dmitienko, V. E. (1989). *Sov. Phys. Usp.* **32**, 697–719.
Brunel, M. & de Bergevin, F. (1981). *Acta Cryst.* A**37**, 324–331.
Cole, H., Chambers, F. W. & Wood, C. G. (1961). *J. Appl. Phys.* **32**, 1942–1945.
Compton, A. H. & Allison, S. K. (1935). *X-rays in Theory and Experiment*. New York: Van Nostrand.
Hart, M. (1978). *Philos. Mag.* B**38**, 41–56.
Hart, M. & Rodrigues, A. R. D. (1979). *Philos. Mag.* B**40**, 149–157.
Hart, M. & Rodrigues, A. R. D. (1981). *Philos. Mag.* B**43**, 321–332.
Hart, M., Siddons, D. P., Amemiya, Y. & Stojanoff, V. (1991). *Rev. Sci. Instrum.* **62**, 2540–2544.
Hirano, K., Ishikawa, T. & Kikuta, S. (1993). *Nucl. Instrum. Methods Phys. Res. A*, **336**, 343–353.
Hirano, K., Ishikawa, T. & Kikuta, S. (1995). *Rev. Sci. Instrum.* **66**, 1604–1609.
Hirano, K., Ishikawa, T., Nakamura, I., Mizutani, M. & Kikuta, S. (1994). *Jpn. J. Appl. Phys.* **33**, L689–L692.
Namikawa, K., Ando, M., Nakajima, T. & Kawata, H. (1985). *J. Phys. Soc. Jpn*, **54**, 4099–4102.
Okitsu, K., Oguchi, T., Maruyama, H. & Amemiya, Y. (1996). *Proc. SPIE*, **2873**, 100–104.
Siddons, D. P., Hart, M., Amemiya, Y. & Hastings, J. B. (1990). *Phys. Rev. Lett.* **64**, 1967–1970.
Sumiya, H., Toda, N., Nishibayashi, Y. & Satoh, S. (1997). *J. Cryst. Growth*, **178**, 485–494.
Templeton, D. H. & Templeton, L. K. (1980). *Acta Cryst.* A**36**, 237–241.
Templeton, D. H. & Templeton, L. K. (1982). *Acta Cryst.* A**38**, 62–67.
Templeton, D. H. & Templeton, L. K. (1985). *Acta Cryst.* A**41**, 133–142.
Zachariasen, W. H. (1945). *Theory of X-ray Diffraction in Crystals*. New York: Wiley.